

Received: 2019.07.21

Accepted: 2019.09.17

Published: 2019.12.19

Multifunctional Polyethylene Glycol (PEG)-Poly (Lactic-Co-Glycolic Acid) (PLGA)-Based Nanoparticles Loading Doxorubicin and Tetrahydrocurcumin for Combined Chemoradiotherapy of Glioma

Authors' Contribution:

Study Design A
Data Collection B
Statistical Analysis C
Data Interpretation D
Manuscript Preparation E
Literature Search F
Funds Collection G

ABCDEF 1,2 **Xingzhen Zhang**
AEFG 1,2 **Lixia Zhao**
AD 2 **Guangxi Zhai**
B 2 **Jianbo Ji**
AFG 1,2 **Anchang Liu**

1 Department of Pharmacy, Qilu Hospital of Shandong University, Jinan, Shandong, P.R. China

2 Department of Pharmaceutics, College of Pharmacy, Shandong University, Jinan, Shandong, P.R. China

Corresponding Author: Anchang Liu, e-mail: acleu@126.com

Source of support: This work was supported by the National Natural Science Foundation of China (No. 81402960), Fundamental Research Funds of Shandong University (No. 2014JC009) and Technology Plan of the Health and Family Planning Commission of Shandong

Background: This study aimed to prepare doxorubicin- and tetrahydrocurcumin-loaded and transferrin-modified PEG-PLGA nanoparticles (Tf-NPs-DOX-THC) for enhanced and synergistic chemoradiotherapy.

Material/Methods: Tf-NPs-DOX-THC were prepared via the double-emulsion method. The morphologies and particle sizes of the prepared nanoparticles were examined by TEM and DLS, respectively. The *in vitro* MTT, apoptosis, and clone formation assays were performed to detect the proliferation and radiosensitivity of cells with various treatments. Cellular uptake assay was also conducted. The tissue distribution of Tf-NPs was investigated by *ex vivo* DOX fluorescence imaging. The *in vivo* tumor growth inhibition efficiency of various treatments was evaluated in orthotopic C6 mouse models and C6 subcutaneously grafted mouse models.

Results: Tf-NPs-DOX-THC exhibited high drug-loading efficiency ($6.56 \pm 0.32\%$) and desirable particle size (under 250 nm). MTT, apoptosis, and clone formation assays revealed the enhanced anti-cancer activity and favorable radiosensitizing effect of Tf-NPs-DOX-THC. Strong fluorescence was observed in the brains of mice treated with Tf-NPs-DOX. The *in vitro* release of drug from nanoparticles was in a pH-sensitive manner. Tf-NPs-DOX-THC in combination with radiation also achieved favorable anti-tumor efficacy *in vivo*.

Conclusions: All results suggest that a combination of Tf-NPs-DOX-THC and radiation is a promising strategy for synergistic and sensitizing chemoradiotherapy of glioma.

MeSH Keywords: **Chemoradiotherapy • Nanoparticles • Receptors, Transferrin**

Abbreviations: **BBB** – Blood–brain barrier; **Cur** – curcumin; **DL** – loading efficiency; **DLS** – dynamic light scattering; **DOX** – doxorubicin; **EE** – encapsulation efficiency; **NPs** – nanoparticles; **RAD** – radiation; **PEG** – polyethylene glycol; **PLGA** – poly (lactic-co-glycolic acid); **SD** – standard deviation; **TEM** – transmission electron microscopy; **Tf** – transferrin

Full-text PDF: <https://www.medscimonit.com/abstract/index/idArt/918899>

 5397

 2

 8

 50


Background

Brain tumors remain a major health problem, with glioma the most commonly occurring and the one that is the most aggressive and with the worst prognosis and the highest mortality rate [1,2]. Although radiotherapy and chemotherapy are 2 treatment types for all cancers, malignant glioma is rarely cured with only chemotherapy or radiotherapy. As a new therapeutic modality, a combination of chemotherapy with radiotherapy has been widely reported to achieve effective treatment of glioma [3–5]. While a synergistic combination of chemotherapy with radiotherapy has become a standard treatment, there are still many factors that restrict therapeutic efficacy [6]. Firstly, many patients may ultimately have to terminate radiotherapy due to the severe radiation-related risks. Additionally, it is difficult to achieve the required concentration of chemotherapeutics in the brain due to the presence of the blood–brain barrier (BBB) [7]. Effective strategies for radiochemotherapy are urgently needed, and the best strategy is to sensitize glioma cells to radiation by increasing the killing of glioma cells per dose of radiation using radiosensitizers [8]. Moreover, nanoparticles modified with targeting ligands have also been developed to improve chemotherapeutic efficacy [9].

Recently, curcumin (Cur) has been widely studied for its radiosensitizing potential in many tumors such as glioblastoma multiform, human oral squamous cell carcinoma, and colorectal cancers [10,11]. Tetrahydrocurcumin (THC), a major active metabolite of curcumin, has also been reported to have potent bioactivity both *in vitro* and *in vivo* [12–14]. Our previous research has confirmed that tetrahydrocurcumin is a potential radiosensitizer for C6 cells; THC sensitized C6 cells to radiation through its effects on cell proliferation, cell apoptosis, cell migration, and cell cycle distribution [15].

Doxorubicin (DOX), one of the most widely used chemotherapeutic drugs, has been used to treat various cancers (e.g., gastric cancer, lung cancer, and breast cancer) by inhibiting DNA replication and RNA transcription [16–19]. However, endothelial tight junctions of the BBB prevent the delivery of free DOX from the blood circulation into the brain, resulting in insufficient drug concentration in the brain and poor therapeutic efficacy in the treatment of glioma [20,21]. In consequence, a higher dose is required to achieve desirable drug concentrations in the brain, ultimately leading to severe adverse effects, especially cardiotoxicity [22]. Recently, targeted ligands-modified nanotechnology has exhibited efficient drug delivery to the tumor site and has been widely applied to enhance chemotherapeutic efficacy and attenuate adverse effects [23–25].

In recent decades, an increasing number of multifunctional nanoparticles (NPs) have been designed to deliver multiple chemotherapeutics simultaneously [26]. Furthermore, nanoparticles

have been constructed and explored for synergistic combination of radiotherapy and chemotherapy by simultaneously delivering chemotherapeutic agents and radiosensitizers [27]. For example, core/shell nanoparticles containing gold NPs and DOX have been developed by Kim et al. and were demonstrated to have significant anti-tumor efficacy [4]. Over the past few decades, various types of materials, synthetic or natural, have been applied as drug delivery carriers, with PEG-PLGA an excellent choice due to its biocompatibility and safety [28]. Additionally, surface modification with PEG has also been reported to protect nanoparticles from phagocytosis by the reticuloendothelial system and exhibit prolonged circulation time in the bloodstream [29].

Drug accumulation and uptake in the brain is greatly limited due to the existence of the BBB, resulting in reduced therapeutic efficacy of glioma [30]. To solve this problem, receptor-mediated endocytosis achieved by coupling nanoparticles with specific ligands is a useful approach. Transferrin receptors (TfR) are highly expressed on the surfaces of brain capillary endothelial cells and glioma cells, and are generally expressed at low levels in most normal tissues [31,32]. Ligand-targeting TfR could be a good choice for the treatment of glioma [33]. Many studies have reported that transferrin (Tf)-conjugated nanoparticles can increase drug concentrations in tumor cells and reduce non-specific toxicity by TfR-mediated endocytosis. In one study, transferrin-modified nanoparticles were demonstrated to be efficient in delivering siEGFR into U87 glioma cells through TfR-mediated internalization, resulting in an enhanced inhibition of tumor proliferation [34]. Recently, smart nanoparticles, which can respond to physical and chemical stimuli such as pH and temperature, have been also developed for the enhanced delivery of anti-cancer drugs [35,36]. In particular, pH-sensitive PLGA hollow microspheres showed a faster release of their cargoes in an acidic solution compared to that in pH 7.4 [37].

In the present study, DOX and THC-loaded transferrin-modified PEG-PLGA nanoparticles (Tf-NPs-DOX-THC) with pH sensitization effects were designed for synergistic chemoradiotherapy of glioma. We describe the design, preparation, and characterization of Tf-NPs-DOX-THC in detail. Furthermore, we evaluated the anti-tumor efficacy of Tf-NPs-DOX-THC combined with radiation both *in vitro* and *in vivo*.

Material and Methods

Materials

DOX was purchased from Shanghai Macklin Biochemical Technology Co. and THC with a purity of 95% was obtained from Xiya-Reagent (China). Maleimide-poly (ethylene glycol) (Mal-PEG, MW 2000 Da) was obtained from Jenkem

Technology (Beijing, China). Methoxy-poly (ethylene glycol)-poly (lactic-co-glycolic acid) (MePEG2000-PLGA20000 (50: 50)) copolymer and maleimide-poly (ethylene glycol) poly (lactic-co-glycolic acid) (Mal-PEG2000-PLGA20000 (50: 50)) copolymer were custom-synthesized by Jinan Daigang Biotechnology Co. Transferrin was purchased from Shanghai Yuanye Biotechnology Co. (China), 2-iminothiolane hydrochloride (2-IT) was obtained from Sigma-Aldrich (St. Louis, MO, USA), Dulbecco's modified Eagle's medium (DMEM) was from HyClone (Gaithersburg, USA), and RPMI-1640 medium was purchased from Thermo Fisher Scientific Co. (China). Fetal bovine serum (FBS) was acquired from TBD Biotechnology Development. Annexin V-FITC and propidium iodide (PI) cell apoptosis kits were purchased from Sungene Biotech Co. 4,6-diamidino-2-phenylindole (DAPI) was purchased from Genview (FL, USA). Plastic cell culture dishes, plates, and flasks were obtained from Corning Inc. (Lowell, MA, USA). Double-distilled water was purified using the Millipore Simplicity System (Millipore, Bedford, MA, USA). All chemicals used were of analytical or chromatographic reagent quality and were purchased from commercial sources.

Cell culture

The rat C6 glioma cell line and human breast cancer cell line (MCF-7) were obtained from the Institute of Biochemical and Biotechnological Drugs of Shandong University. The human glioma U251 cell line was kindly provided by the Institute of Brain Science Research, Qilu Hospital of Shandong University. The U251 cells line and C6 cells line were cultured in DMEM containing 10% FBS. MCF-7 cells were incubated in RPMI 1640 medium containing 10% FBS. All cells were maintained in a humidified incubator in an atmosphere of 5% CO₂ and 95% air.

Animals

Kunming mice (18–22 g, ♂) were obtained from Jinan Peng Yue Experimental Animal Breeding Co. (Shandong, China). Nude mice (18–20 g, ♂) were purchased from Nanjing Biomedical Research Institute of Nanjing University (Nanjing, China). The animals were kept on a 12-h light–dark cycle with free access to food and water. All protocols involving animal handling were in compliance with the China Animal (Scientific) Procedures Act.

Preparation and characterization of NPs-DOX-THC and Tf-NPs-DOX-THC

Preparations of NPs-DOX-THC

Hydrophobic doxorubicin was prepared as described previously [38]. NPs-DOX-THC were prepared by a double-emulsion method. First, 0.3 ml of water containing NaHCO₃ (2.5 mg/ml) was emulsified with 2 ml dichloromethane containing 15 mg

MPEG-PLGA, 1 mg doxorubicin, and 1 mg tetrahydrocurcumin. The emulsification was performed using a probe sonicator at 120 W for 4 min in an ice bath. Then, the primary emulsion and 2 mL of 2% polyvinyl alcohol (PVA) were emulsified by sonication for 6 min to form the W/O/W emulsion, which was further dropped into 0.6% PVA solution and stirred overnight at room temperature to evaporate the dichloromethane. The final mixture was centrifuged at 4000 rpm for 10 min and the supernatant was filtered through a 0.8-μm membrane to remove unloaded drugs. The DOX-loaded nanoparticles (NPs-DOX) and THC-loaded nanoparticles (NPs-THC) were prepared as described above with only the addition of THC or DOX into the dichloromethane solution.

Preparations of Tf-NPs-DOX-THC

Nanoparticles conjugated with transferrin (Tf-NPs-DOX-THC) were prepared by maleimide-thiol coupling reaction [23]. Tf was thiolated and purified as described previously [39,40]. Then, the purified thiolated transferrin (Tf-SH) was added to NPs and incubated under a nitrogen atmosphere at room temperature for 9 h to prepare the Tf-NPs. MAL-PEG-PLGA: Tf at a molar ratio of 1: 3 was employed in the reaction. The resulting Tf-NPs were then subjected to a sepharose CL-4B column and eluted with 0.01 M phosphate-buffered saline (PBS) to remove the unconjugated thiolated transferrin. The eluate was collected and the conjugation efficiency of transferrin was tested using a BCA kit.

Characterization of NPs-DOX-THC and Tf-NPs-DOX-THC

The particle size and zeta potential of nanoparticles were analyzed by Malvern Zetasizer Nano-ZS90 dynamic light scattering (DLS) (Malvern Instruments, UK). The morphologies of nanoparticles were examined by transmission electron microscopy (TEM; JEM-100CX II, Japan). The samples were dropped onto a copper grid, stained with 2% (w/v) phosphotungstate solution for 20 s, and air-dried.

To quantify drug-loading efficiency (DL) and encapsulation efficiency (EE) of NPs, a predetermined amount of NPs was dissolved in acetonitrile. The THC level was determined with an Agilent 1220 HPLC system (Agilent Technologies, Germany) using a Hypersil-BDS C18 column. The mobile phase was acetonitrile: 5% (V/V) glacial acetic acid in water (45: 55), with a flow rate of 1.0 ml/min, and the detection wavelength was set at 280 nm. The concentration of DOX was monitored using a Visible-UV spectrophotometer at 480 nm. The EE% and DL% of DOX and THC in the NPs were calculated according to the equations below [41]:

$$EE\% = \frac{W_{\text{loaded}}}{W_{\text{added}}} \times 100\%$$
$$DL\% = \frac{W_{\text{loaded}}}{W_{\text{total}}} \times 100\%$$

Where W_{loaded} represented drug loaded in the nanoparticles, W_{added} was the initially added amount of drug, and W_{total} was the amount of both drug and polymer in the nanoparticles.

In vitro drug release

The *in vitro* drug release assay was designed based of the method described in a previous study to verify the pH-responsive characteristics of the NPs [37]. For this, 2 ml of drug-loaded nanoparticles were placed into a dialysis bag (MWCO: 3500 Da, Solarbio), which was immersed in 40 ml of phosphate buffer (pH 5.0 and 7.4, 10 mM, containing 1.0% Tween 80). The release medium was then incubated in a shaking water bath maintained at 37°C and shaken horizontally at 100 rpm. At predetermined time intervals, a specified amount of medium was withdrawn and an equal volume of fresh phosphate buffer was added to maintain sink conditions. The quantification of released DOX was evaluated by fluorescence spectrophotometry (F-7000, Hitachi, Japan), measuring the absorbance at excitation/emission of 470/557 nm. The released THC was quantified using HPLC.

In vitro cytotoxicity

The cytotoxicity study was performed by the conventional 3-(4, 5-dimethylthiazol-2-yl)-2, 5-diphenyltetrazolium bromide (MTT) reduction assay. Briefly, C6 cells were seeded in 96-well plates at a density of 5000 cells/well in 100 μ l growth medium. After 24-h incubation, the cells were treated with various concentrations of blank nanoparticles, free DOX, NPs-DOX-THC, and Tf-NPs-DOX-THC for different times. Finally, MTT solution was added into each well and the absorbance was detected with a microplate reader (Bio-Rad, California, USA) at a wavelength of 570 nm.

In vitro cellular uptake

Cellular uptake of various nanoparticles was analyzed using a fluorescence microscope. C6 and MCF-7 cells were seeded into 6 well plates (1×10^5 cells/well, respectively and 5×10^4 cells/well) and treated with free DOX, NPs-DOX or Tf-NPs-DOX (containing DOX 10 μ g/ml) for 0.5, 2, and 4 h, respectively. MCF-7 cells were treated with NPs-DOX, Tf-NPs-DOX, or Tf-NPs-DOX+Tf (MCF-7 cells pre-incubated with 100 μ g/ml free transferrin for 30 min) for 0.5 and 4 h. After removal of culture medium, cells were washed with cold PBS, fixed with 4% paraformaldehyde for 15 min, and stained with DAPI for 10 min in the dark. The fluorescence images were taken from a randomly-selected location using a fluorescence microscope (Olympus Corp., Tokyo, Japan)

Apoptosis analysis

For apoptosis analysis, cells were treated with Tf-NPs-THC, NPs-THC, and free THC at a final THC concentration of 20 μ M

for 12 h and then exposed to radiation at 3Gy. At the end of treatment, cells were then stained with Annexin V-FITC and propidium iodide solution for 15 minutes. The fluorescence was assessed by flow cytometry (Bio-Rad, California, USA).

Clonogenic survival assay

C6 and U251 cells in logarithmic growth phase were seeded in 6-well plates at appropriate cell densities. After 12 h of incubation with free THC (20 μ M) or Tf-NPs-DOX-THC, cells were exposed to radiation at increasing doses, from 0 Gy to 8 Gy, using a medical X-ray irradiator (PRIMUS HI, Siemens, Germany) at a dose rate of 300 cGy/min, focus-surface distance of 100 cm, and radiation field size of 40×40 cm. Fourteen days later, cell clones were fixed with 4% paraformaldehyde for 15 min and stained with 0.5% crystal violet in PBS. The plating efficiency (PE) was calculated by dividing the number of clones by the number of cells seeded. The survival fraction (SF) was calculated using the equation: SF=colony numbers/(plating cell numbers×PE). The cell radiation dose survival curve was plotted using X–Y log scatter and fitted with formula of the Single Hit Multi-Target (SHMT) model.

Ex vivo fluorescence imaging

The tissue distribution and brain targeting properties of Tf-NPs-DOX were investigated by *ex vivo* DOX fluorescence imaging according to a previously-described method [4]. Kunming mice received intravenous injection of free DOX or Tf-NPs-DOX at a DOX dose of 5 mg/kg. After 1, 2, 6, and 12 h, mice were sacrificed, and the major organs (heart, liver, spleen, lung, kidney, and brain) were excised carefully for *ex vivo* imaging. *Ex vivo* DOX fluorescence images were captured using the Xenogen IVIS Lumina system (Caliper Life Sciences, USA) with an ICG filter (excitation at 500 nm, emission at 590 nm). The exposure time was set to 5 s. Results were analyzed using Living Image 4.1 software (Caliper Life Sciences, USA).

In vivo anti-glioma efficacy

The *in vivo* tumor growth inhibition was performed on nude mice bearing glioma xenografts. The nude mice were subcutaneously injected with 100 μ l of suspension containing 1×10^7 C6 cells in the armpit of the right anterior limb. After about 7 days, when the volume of tumors reached about 50–150 mm³, mice were randomly divided into 6 groups (5 mice per group) with the following treatments:

- Group 1 (Saline): normal saline (0.9% NaCl);
- Group 2 (RAD+Saline): radiation only;
- Group 3 (RAD+THC): combinational treatment with free THC solution and radiation;
- Group 4 (RAD+DOX): co-treated with free DOX solution and radiation;

Table 1. The effects of formulation parameters on encapsulation efficiency and loading content of drug-loaded nanoparticles.

Copolymer: DOX: THC	DOX (EE%)	DOX (DL%)	THC (EE%)	THC (DL%)
10: 1: 1	44.60±1.32	4.27±0.12	19.82±1.09	1.94±0.10
15: 1: 1	56.11±3.67	3.61±0.23	48.00±1.79	3.10±0.11
25: 1: 1	64.40±5.51	2.51±0.21	63.72±4.36	2.49±0.17
35: 1: 1	85.57±2.95	2.39±0.08	63.72±4.36	2.00±0.04

Table 2. Characterization of drug-loaded PEG-PLGA nanoparticles.

Sample	DL%	EE%	Size (nm)	PDI	Zeta potential(mv)
NPs-DOX	3.97±0.19	61.96±3.06	183.43±1.37	0.34±0.21	-11.67±1.01
NPs-THC	4.60±0.13	74.28±2.10	220.97±3.83	0.29±0.11	-13.90±1.66
NPs-DOX-THC	6.71±0.30	/	239.57±2.53	0.25±0.03	-12.57±0.71
Tf-NPs-DOX-THC	6.56±0.32	/	255.77±6.15	0.24±0.09	-16.80±0.87

Group 5 (RAD+THC/DOX): solution containing free DOX and THC co-treated with radiation;

Group 6 (RAD+Tf-NPs-DOX-THC): co-treated with Tf-NPs-DOX-THC and radiation.

The mice were treated 5 times (on days 1, 4, 7, 10, and 13) with various treatments containing drug at a dose of 5 mg/kg, followed by 3 Gy of radiation. For *in vivo* radiation treatment, a medical X-ray irradiator was used. The tumor volumes and body weights were recorded every day. Tumor volume was calculated by the formula: $V=(W^2 \times L)/2$, where W and L represented the largest and smallest tumor diameters, respectively. Three weeks after implantation, mice were sacrificed and tumors were dislodged and weighed. The major organs were removed for histological examination by HE staining. The tumor inhibition rate was calculated using the following equation: Tumor inhibition rate (%) = $(1 - W_{\text{sample}}/W_{\text{control}}) \times 100\%$. W_{control} and W_{sample} represented the weight of tumors in the control and sample groups at the end of the experiment, respectively.

The anti-tumor efficacy of the formulations was also assessed in nude mice bearing intracranial gliomas. Animal models were prepared by implanting C6 cells (1×10^6 suspended in 10 μ L PBS) into the right caudate nucleus using a stereotaxic instrument. The stereotaxic needle was lowered 2.5 mm and then raised 0.5 mm perpendicular to the hole to prevent reflux of C6 cells [2]. After 7 days of xenograft glioma, mice were randomly divided into 5 groups and received saline, RAD+saline, RAD+THC, RAD+DOX/THC, or RAD+Tf-NPs-DOX-THC every other day. Two weeks later, mice were euthanized. Brains were collected and fixed with 4% paraformaldehyde at 4°C overnight, and then sectioned for hematoxylin and eosin (HE) staining.

Statistical analysis

Data are expressed as means±standard deviation (SD). All data were statistically analyzed with SPSS software (version 17.0) using single-factor analysis of variance (one-way ANOVA) followed by the least significant difference (LSD) post hoc tests. A difference with a p value less than 0.05 was considered statistically significant.

Results

Preparation and characterization of drug-loaded nanoparticles

The HPLC measurement of free DOX and NPs-DOX-THC showed that both DOX and THC had been successfully encapsulated into nanoparticles and separated completely (Supplementary Figure 1). Taking DL% and EE% as the index, single-factor experiments were conducted to optimize preparation technology. As can be seen in Table 1, DL% and EE% were evidently changed along with varying the mass ratio of drug to copolymer. The highest encapsulation efficiencies of THC and DOX in nanoparticles were 63.72±4.36% and 85.57±2.95%, respectively, at a copolymer/drug ratio of 35: 1: 1. When the copolymer/drug ratio was 15: 1: 1, nanoparticles presented a desirable drug-loading content of 6.71±0.30%. Taking both DL% and EE% into consideration, the copolymer/drug ratio of 15: 1: 1 was selected for further research. The modification of Tf barely affected the total drug-loading content (6.56±0.32%). Furthermore, when compared with the single-drug delivery system, the combined drug-delivery system exhibited a higher total drug-loading content (Table 2).

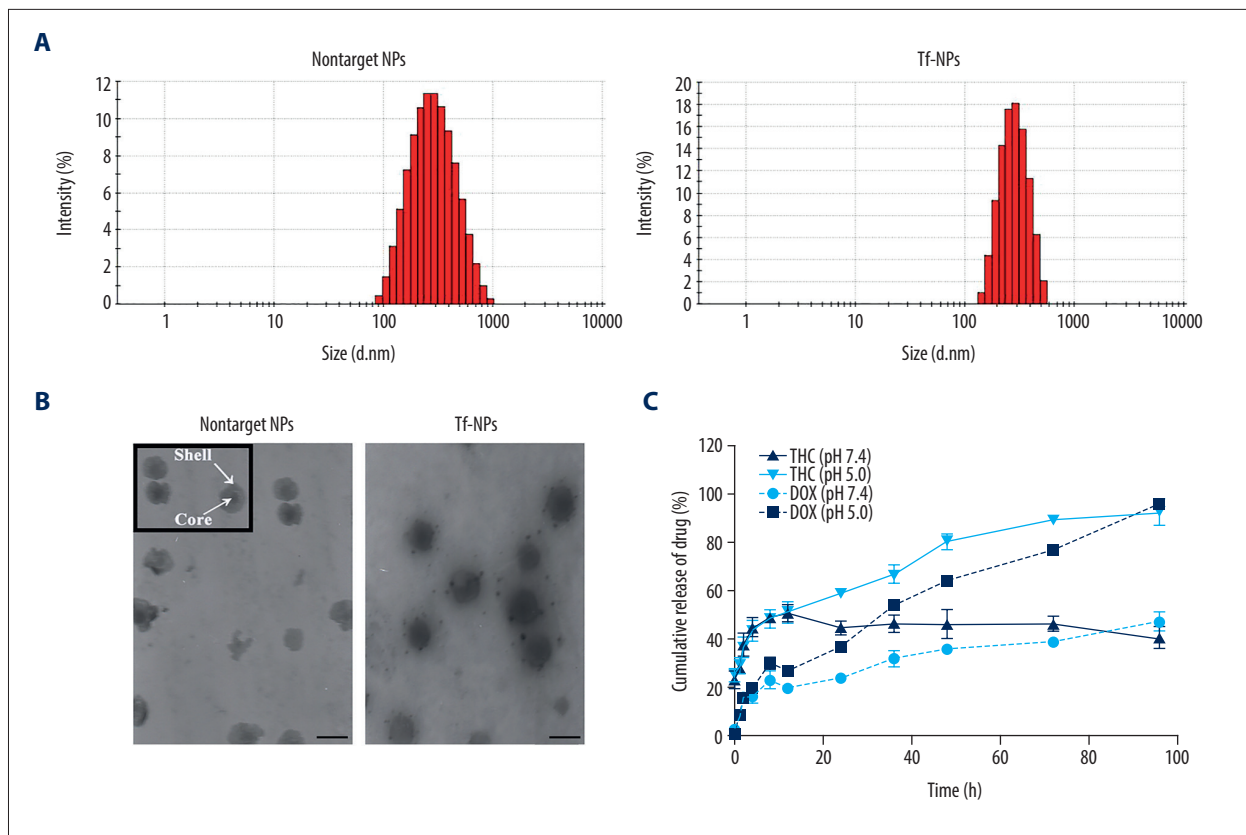


Figure 1. (A) Size distribution of non-targeted nanoparticles and transferrin-targeted nanoparticles was determined by DLS. (B) TEM images showed the morphology of nontarget NPs and Tf-NPs. Inset: Core-shell structure of nanoparticles (scale bar: 200 nm). (C) *In vitro* release profiles of DOX and THC from nanoparticles in different pH (pH: 7.4, pH: 5.0). Data are expressed as the mean \pm SD (n=3).

The size distribution, zeta potential, and polydispersity index (PDI) of various drug-loaded formulations are shown in Table 2. The mean particle size of each formulation characterized by DLS was around 200 nm, with a polydispersity index of less than 0.3, indicating that the prepared nanoparticles were uniform. As shown in Figure 1A, the sizes of the nanoparticles conjugated with transferrin were slightly increased (239.57 ± 2.53 nm for NPs-DOX-THC and 255.77 ± 6.15 nm for Tf-NPs-DOX-THC). Tf-modified nanoparticles demonstrated an increased zeta potential compared with NPs, which can be attributed to the anionic characteristics of Tf.

The morphology of nanoparticles was investigated by TEM (Figure 1B). The fabricated nanoparticles were spherical and homogeneously distributed, with a defined core-shell structure. The active ligand Tf on the nanoparticle surface ensured the targeting effects of Tf-NP to the Tf receptor, and the conjugation efficiency of Tf detected by the BCA kit was 32.5%.

***In vitro* drug release**

As depicted in Figure 1C, only $41.18\pm 5.94\%$ of THC and $36.73\pm 2.28\%$ of DOX were released during the first 48 h of incubation at pH 7.4. In comparison, for nanoparticles incubated at pH 5.0, $80.23\pm 3.17\%$ of THC and $66.88\pm 3.55\%$ of DOX were released after 48 h. During 96 h of incubation, no more than 50% of drugs were cumulatively released at pH 7.4, while the cumulative release percentage of THC and DOX at pH 5.0 was $92.33\pm 5.31\%$ and $97.96\pm 3.05\%$, respectively.

***In vitro* cytotoxicity**

The cytotoxicity of nanoparticles was evaluated by MTT assay in C6 cells, with doxorubicin (DOX) used as a control. As shown in Figure 2A, blank nanoparticles showed little cytotoxicity to C6 cells and their cell viability was more than 90% even at a high concentration corresponding to 400 μ g/mL of PEG-PLGA. From Figure 2B and 2C, it can be seen that both free DOX and drug-loaded nanoparticles showed a dose-dependent and time-dependent cytotoxicity against C6 cells. NPs-DOX-THC exhibited slightly lower cell inhibition efficiency than free DOX at the

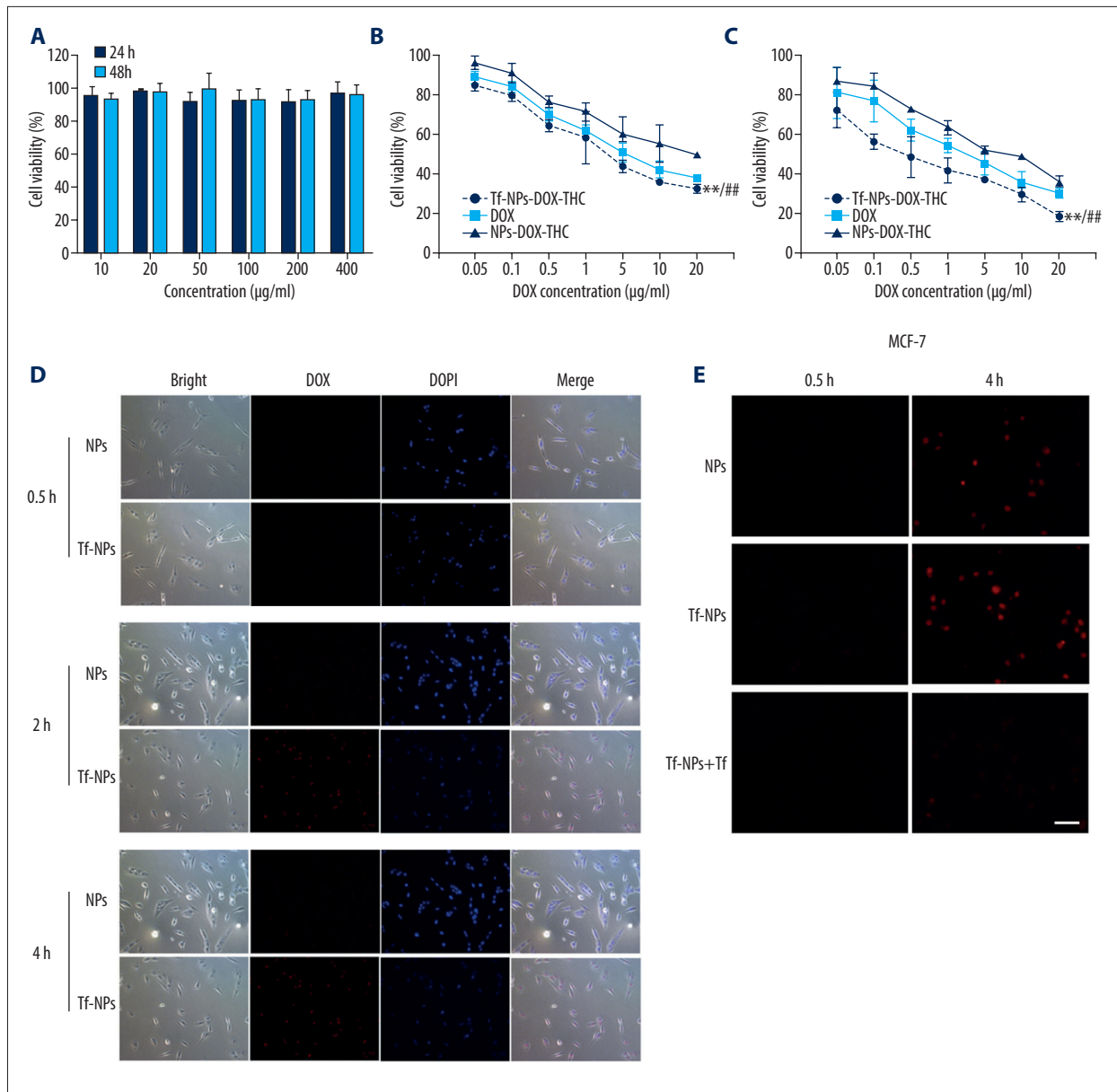


Figure 2. (A) Cell viabilities of C6 cells cultured with various concentrations of blank polymeric nanoparticles for 24 h and 48 h. Cytotoxicity of free DOX, NPs-DOX-THC and Tf-NPs-DOX-THC on C6 cells with 24-h (B) and 48-h (C) incubation. (D) The cellular uptake of NPs-DOX and Tf-NPs-DOX was shown using a fluorescence microscope images in C6 cells. (E) Confocal images of MCF-7 cells incubated with NPs-DOX, Tf-NPs-DOX and Tf-NPs-DOX +Tf for 0.5 and 4 h. Cell nuclei were stained blue with DAPI (10 µg/ml) and DOX is shown as red fluorescence. The scale bar is 100 µm. Data are expressed as the mean±SD (n=4); ** p<0.01 vs. DOX group; ## p<0.01 vs. NPs-DOX-THC group.

same concentration, while transferrin-targeted nanoparticles exhibited enhanced cell-killing ability compared with free DOX. Compared with NPs-DOX-THC, transferrin-targeted nanoparticles inhibited C6 cell growth more significantly ($p<0.01$), indicating that the cellular uptake of nanoparticles by C6 cells was promoted by modification of transferrin.

In vitro cellular uptake

According to the fluorescence images (Figure 2D), the fluorescent intensities of nanoparticles in C6 cells were much stronger after 4-h incubation than in the first 0.5 h, indicating that the cellular uptake of nanoparticles occurred in a time-dependent manner via the endocytosis process. A slight fluorescence was detected in cells incubated with non-targeted nanoparticles,

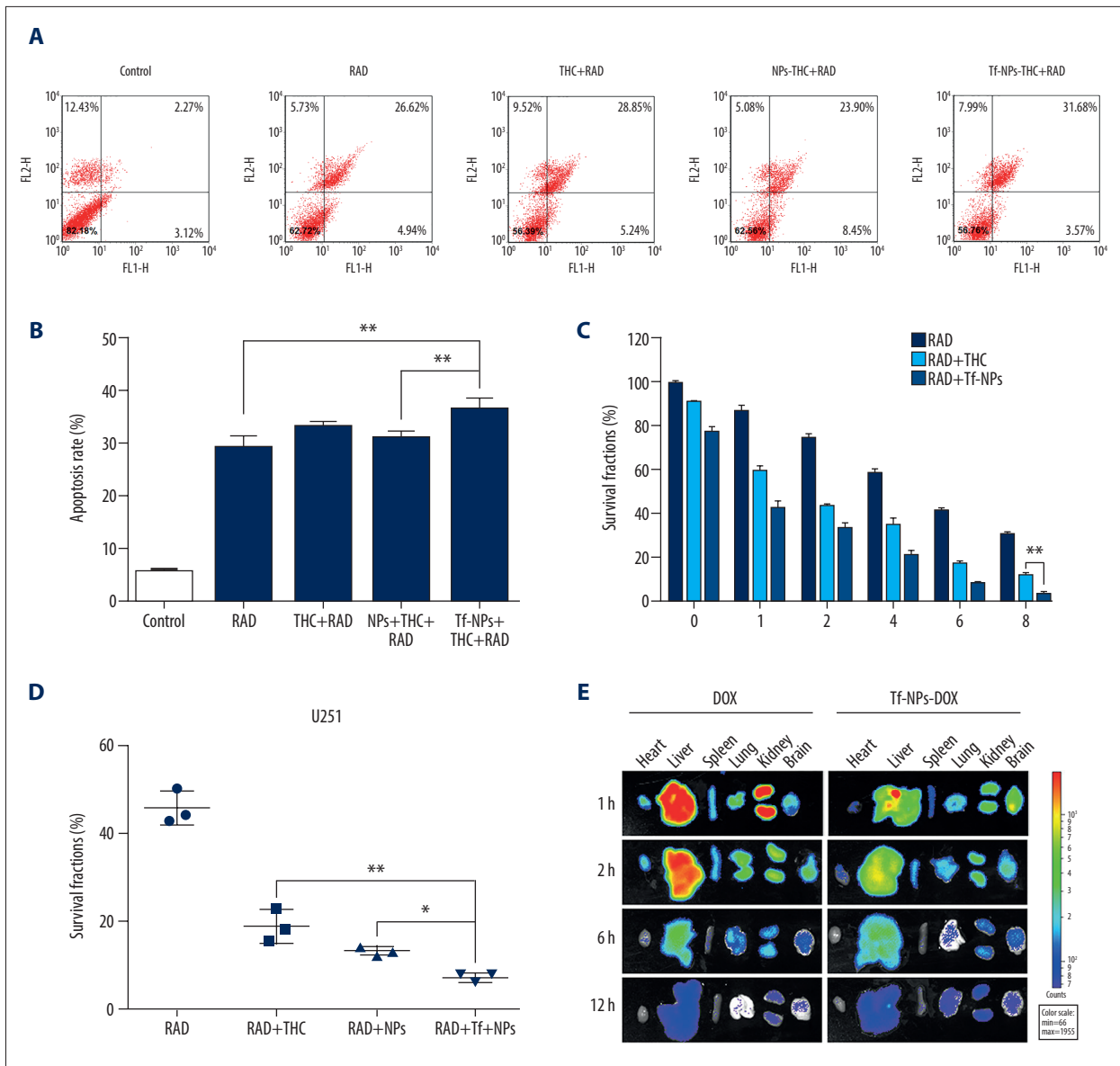


Figure 3. (A) After treatment with PBS, THC, NPs-THC, and Tf-NPs-THC for 12 h, C6 cells were exposed to radiation at doses of 3 Gy and subjected to a flow cytometry assay. (B) Quantification of cell apoptotic rates was also calculated. (C) Survival curve of C6 cells incubated with PBS, THC, and Tf-NPs-DOX-THC for 12 h (the concentration of THC was 20 μ M), before being treated with various doses of radiation. (D) Surviving fraction of U251 cells in various treatment groups. (E) DOX distribution in various organs after intravenous administration of free DOX and Tf-NPs-DOX measured at 1, 2, 6, and 12 h following injection. Data are expressed as the mean \pm SD from 3 independent experiments (* p <0.05, ** p <0.01).

whereas much higher fluorescence intensities were observed in cells treated with transferrin-targeted nanoparticles, suggesting that transferrin-targeted nanoparticles showed higher and faster cellular uptake than non-targeted nanoparticles. In addition, after 2 h of incubation, cells treated with drug-loaded nanoparticles showed fluorescence in both cell cytoplasm and nuclei, showing the successful drug release from nanoparticles in the C6 cells.

As presented in Figure 2E, cells treated with transferrin-targeted nanoparticles also showed a higher fluorescence intensity compared with the NPs group in MCF-7 cells. However, after being pre-incubated with free transferrin, the fluorescence intensity from the transferrin-targeted nanoparticles sharply fell. The fabricated nanoparticles, Tf-NPs, are mainly taken up by TfR-mediated endocytosis. Consequently, incubation with free transferrin resulted in a partial blockade of TfR, leading to competitive inhibition of the uptake of Tf-NPs by MCF-7 cells.

Apoptosis analysis

As depicted in Figure 3A and 3B, the control group showed very little apoptosis of C6 cells. The percentages of apoptosis (including early and late apoptosis) in the NPs-THC+RAD and Tf-NPs-THC+RAD groups were $31.16 \pm 1.12\%$ and $36.89 \pm 1.65\%$, respectively. It was evident that Tf-NPs-THC+RAD treatment caused greater apoptosis in the C6 cells as compared to the NPs-THC+RAD group and THC+RAD group.

Clonogenic survival assay

To evaluate the radiotherapy sensitivity of glioma cells treated with various formulations containing THC, colony formation assay was conducted in C6 cells and U251 cells. As presented in the survival curves (Figure 3C, 3D), the surviving fractions showed a significant decrease when cells were treated with THC before radiation, indicating that THC sensitized the C6 cells to radiation. Moreover, the survival rates of C6 and U251 cells in Tf-NPs-DOX-THC +RAD groups were much lower than those in THC+RAD groups ($p < 0.01$), probably due to the synergistic effect of combined radiotherapy and chemotherapy and enhanced cellular uptake.

Ex vivo fluorescence imaging

As shown in Figure 3E, the brains of the mice treated with transferrin-targeted nanoparticles exhibited superior fluorescence efficiency (8.380×10^4) to that of DOX solution-treated mice (5.031×10^4) at 1 h after administration. After 12 h, the fluorescence intensity of the brains in the Tf-NPs-DOX group (2.268×10^4) was nearly twice that in the free DOX group (1.267×10^4). The highest drug accumulations of Tf-NPs-DOX and free DOX solution were observed in the liver, indicating that DOX was mainly metabolized there. The hearts of the mice in the free DOX group exhibited a stronger DOX signal compared with those in the Tf-NPs-DOX group.

In vivo anti-glioma efficacy

The ultimate goal of this study was to investigate whether Tf-NPs-DOX-THC combined with radiation could further improve the therapeutic efficiency and inhibit the growth of glioma *in vivo*. In this study, both orthotopic C6 glioma models and C6 subcutaneously grafted mouse models were established. The C6 subcutaneously grafted mouse models were established by injecting C6 cells into the right axillary of nude mice. Tumor growth in mice was a critical index for the evaluation of anti-tumor efficacy (Figure 4A, 4B). Tumors in control animals grew rapidly, from $131.40 \pm 54.72 \text{ mm}^3$ on initial day to $3257.35 \pm 962.25 \text{ mm}^3$ on day 15. Notably, the combined therapy of THC and RAD showed clear suppression of tumor growth compared with the saline group, suggesting that THC was effective at tumor sensitization to RAD. Moreover, the tumor

suppression of RAD+THC/DOX was significantly stronger than that of RAD+THC, which can be attributed to the good synergistic anti-tumor efficiency of the combined radiotherapy and chemotherapy. Of note, in comparison with RAD+THC/DOX, RAD+Tf-NPs-DOX-THC suppressed tumor growth more strongly during the treatment period ($p < 0.01$), which could be attributed to the high biocompatibility of carrier materials, active targeting efficiency, and appropriate diameter of nanoparticles for the EPR effect at the tumor site. At the end of the treatment, mice were sacrificed and tumors were collected and weighed to calculate tumor inhibition rate (TIR), shown as Figure 4D. Consistent with the above results, RAD+Tf-NPs-DOX-THC showed the lowest tumor weight ($0.19 \pm 0.07 \text{ g}$) and highest TIR% (94.49%) compared with other treatments. All of these results confirmed the good anti-tumor efficacy of the combined therapy with DOX, THC, and RAD. Changes in mouse body weights were also monitored, and the body weight in all treatments showed a slight increase, but with no statistically significant difference (Figure 4C). However, while mice in the saline and free DOX groups became thinner, their body weights actually increased due to their growing tumor volume.

At the end of the experiment, histological analysis of the hearts, livers, spleens, lungs, kidneys, and brains were conducted to perform a safety evaluation. The results showed that there were almost no visible histopathological changes and no damage to the major organs in the RAD+Tf-NPs-DOX-THC group as compared with that in the control group, suggesting the safety of the combined therapy for *in vivo* application (Figure 4E).

To further evaluate the anti-glioma efficacy, orthotopic C6 glioma models were established by stereotactic intracranial injection into the right striatum with 1×10^6 C6 cells before treatment in various groups every other day. The examination of brain sections in orthotopic C6 glioma mice revealed greater presence of tumor mass compared with the brain sections of normal mice (Supplementary Figure 2). From Figure 5A, it can be seen that the tumor volume was greatly reduced in mice treated with RAD+Tf-NPs-DOX-THC as compared with the other 4 groups. The tumor inhibition rate in the mice treated with RAD+Tf-NPs-DOX-THC was 2.15-fold, 1.21-fold, and 1.15-fold higher than in those treated with RAD+saline, RAD+THC, and RAD+THC/DOX, respectively (Figure 5B). These results are consistent with the inhibitory effects seen in C6 subcutaneously grafted mice, suggesting that RAD+Tf-NPs-DOX-THC was exceedingly effective at inhibition of glioma growth due to combined radiotherapy and chemotherapy.

Discussion

Although combined chemo-/radiotherapy has been widely applied as a standard strategy in treating malignant brain glioma,

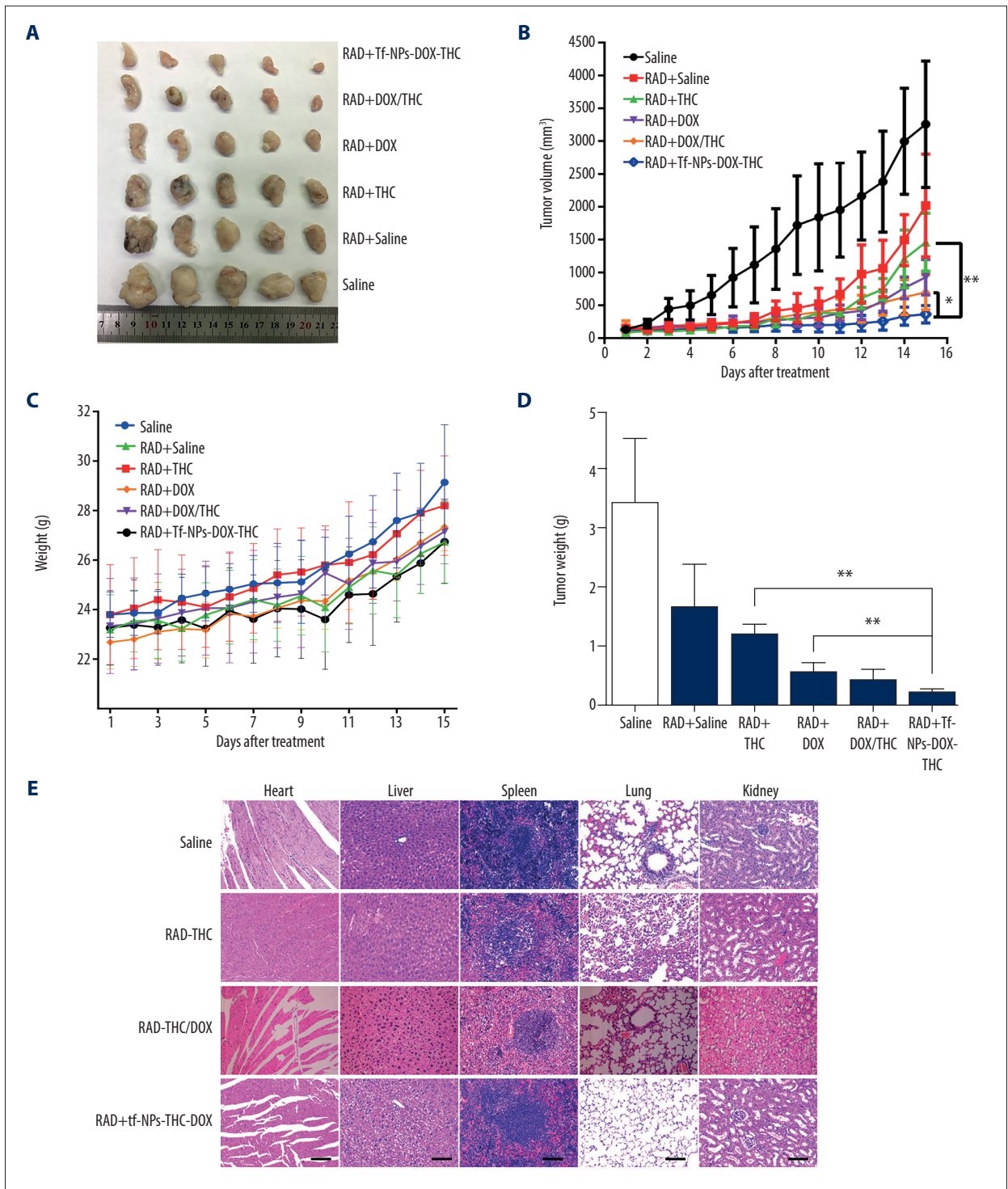


Figure 4. Therapeutic efficacy of various groups in C6 cells xenograft models. **(A)** Macroscopic images of tumors removed from the sacrificed mice on day 15. Tumor volume **(B)** and body weight **(C)** were measured daily after treatment. **(D)** Tumor weight at the end of study. **(E)** HE staining of major organs (heart, liver, spleen, lung, kidney, and brain) after treatment. Scale bar: 100 μ m. Data are presented as the mean \pm SD (n=5, * p<0.05, ** p<0.01).

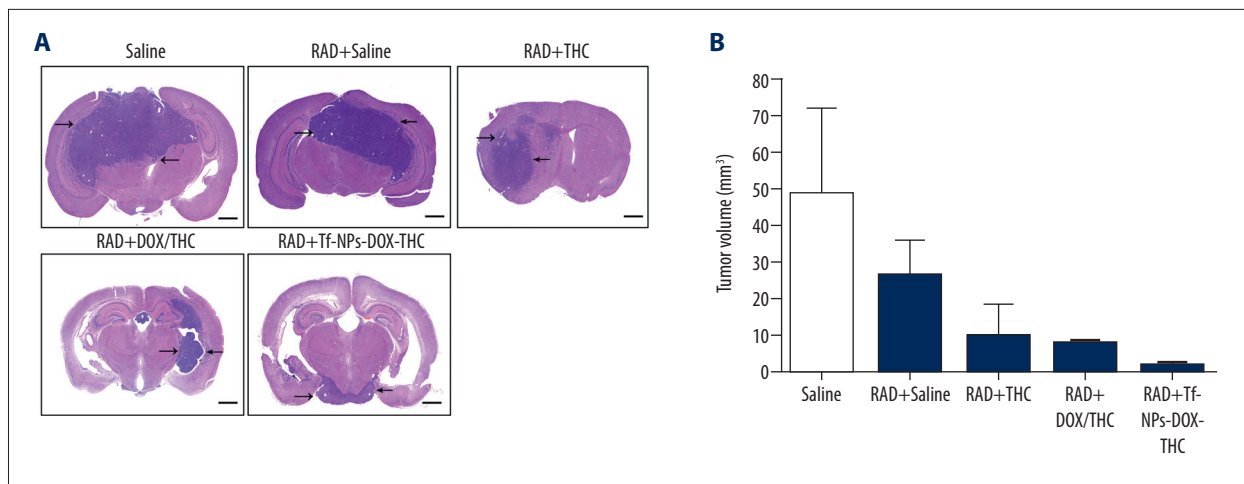


Figure 5. The anti-tumor efficacy of various treatments in nude mice bearing intracranial gliomas. (A) Representative scanning pictures of HE staining of brain sections after various treatments. Arrows indicate the tumor edge. Scale bar: 1000 μm . (B) Tumor volumes were calculated at the study end-point. Data are presented as mean \pm SD.

there are still challenges in achieving optimum and successful treatment of glioma. One of the obstacles is the low chemotherapeutic agent penetration across the BBB and insufficient drug accumulation in tumor sites due to the BBB [4]. The other critical impediment is radiotherapy-related adverse effects due to the high radiation dose used in highly aggressive sub-populations [42]. Therefore, in this study, we aim to develop a brain targeting and radiation-sensitized nanoparticle carrying DOX and THC to achieve synergetic and improved chemo-/radiotherapy for glioma. THC was performed as a radiosensitizer. The therapeutic efficacy of these synthesized multifunctional nanoparticles was evaluated *in vitro* and *in vivo*.

DOX and THC were simultaneously encapsulated in the hydrophobic layer of PEG-PLGA by the double-emulsion method, as shown in Figure 6. First, a two-step emulsion process was performed to prepare a water-in-oil-in-water emulsion. After the evaporation of organic solvent, transferrin was conjugated to the surface of nanoparticles by maleimide-thiol coupling reaction. As shown in Figure 1A, the size of the nanoparticles conjugated with transferrin was slightly increased, which suggested successful conjugation of Tf on NPs. The fabricated nanoparticles showed a desirable diameter of 200 nm and a negative zeta potential. It has been proved that particle size and zeta potential play a crucial role in the pharmacokinetics and cell internalization of nanoparticles. Generally, nanoparticles with diameter around 200 nm are reported to be easily phagocytosed by the brain capillary cells and tend to penetrate into tumor sites via the enhanced permeability and retention (EPR) effect [43]. In addition, the negative zeta potential can result in a decrease in the plasma protein adsorption of nanoparticles and an increase in the stability of the drug delivery system due to the electrostatic repulsive-force [44,45].

The cumulative drug release from nanoparticles was implemented in different PBS solutions (pH 5.0 and 7.4), correspondingly simulating the microenvironment of the endosome-lysosome in carcinoma cells and the human normal tissues or blood, respectively [46]. The cumulative release profiles (Figure 1C) indicated that the prepared nanoparticles displayed lysosomal-targeted release behavior and could prevent the initial drug burst during blood circulation after administration due to the inferior release profile at pH 7.4 and accelerated release characteristics at pH 5.0. We speculate that when NPs are delivered into the lysosome, protons could rapidly diffuse through the free volume in the PLGA shells to react with NaHCO_3 and form a large number of CO_2 bubbles, promoting the degradation of the core-shell structure of nanoparticles [37]. In addition, similar release profiles obtained from both DOX and THC provided a possibility of concurrent radiotherapy and chemotherapy.

For the *in vitro* cytotoxicity experiments, natural DOX resulted in a higher cytotoxicity as compared to the NPs-DOX-THC (Figure 3B, 3C). This phenomenon was previously observed by Cui et al. [47]. It has been reported that free DOX can be easily transported into cells via passive diffusion without energy support, whereas nanoparticles are internalized into cells by endocytosis. In addition, the controlled and incomplete release of the drug from nanoparticles in tumor cells can also lead to lower cell inhibition efficacy [48,49]. In contrast, the *in vitro* cytotoxicity can be upregulated by modifying the NPs with Tf, as cell viability in the Tf-NPs-DOX-THC group was even lower than that in the natural DOX group, which may be attributed to the increased cellular uptake by C6 cells and a combined *in vitro* anti-proliferation effect of THC and DOX.

Due to the high affinity between Tf with TfR, the enhanced endocytosis mediated by Tf can be achieved even with a low Tf

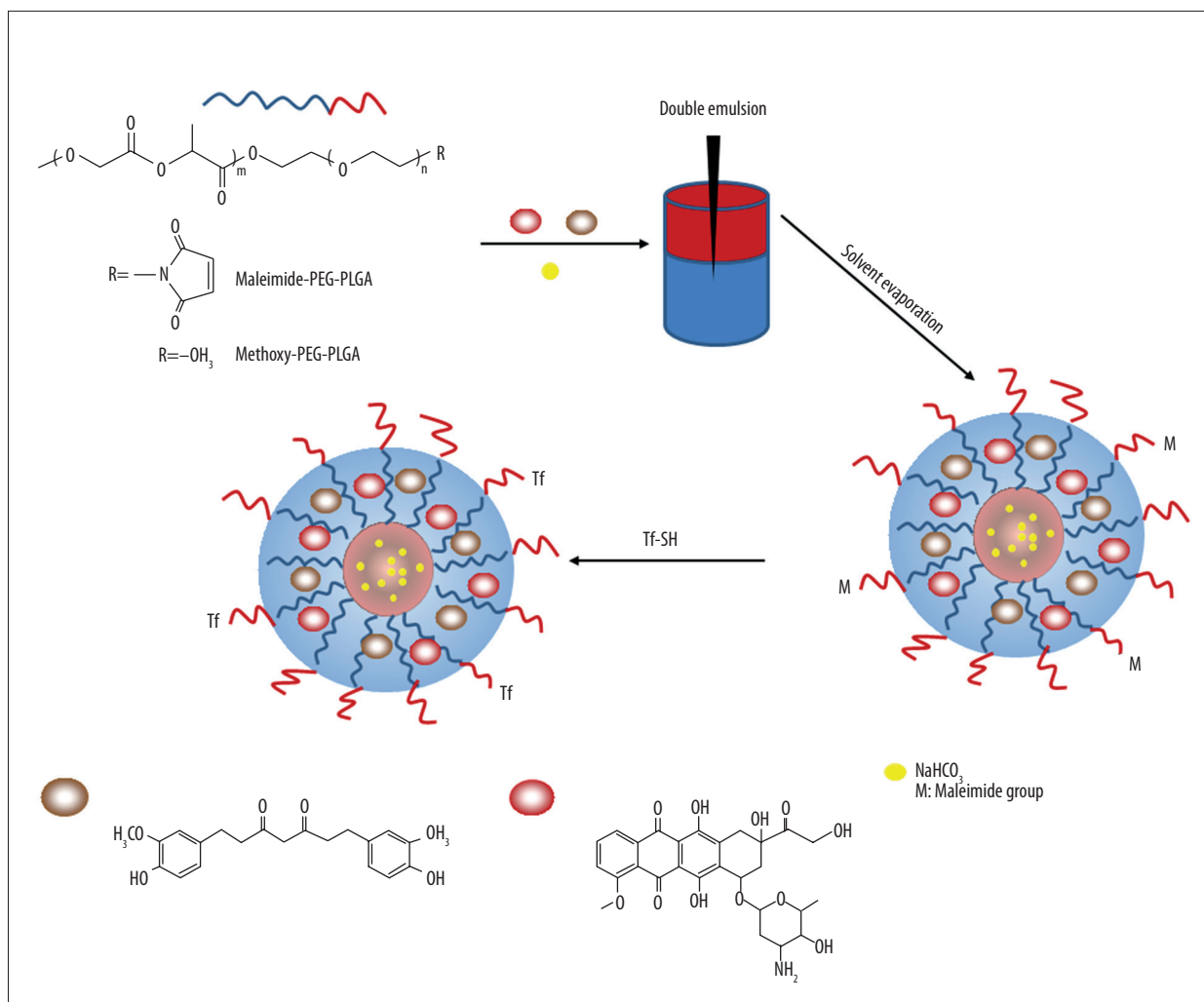


Figure 6. Schematic was used to illustrate the preparation of Tf-NPs-DOX-THC.

conjugation rate on the surface of NPs [50]. C6 cells and MCF-7 cells were used as cell models, since transferrin receptors were seen to be highly expressed in both C6 cells and MCF-7 cells. The internalization of various formulations in C6 cells and MCF-7 cells was visualized by fluorescent inverted microscope (Figure 2D, 2E). The uptake of NPs was enhanced by the modification of Tf, which may be due to specific ligand-receptor interaction involving transferrin. These results are in accordance with cytotoxicity studies in which Tf-targeted NPs were demonstrated to achieve a higher cytotoxicity compared with non-targeted NPs.

Interestingly, Tf-NPs-THC+RAD treatment showed a higher efficiency of apoptosis induction in C6 cells as compared to the THC+RAD group (Figure 3A, 3B), indicating that THC cellular internalization can be enhanced via encapsulating THC into nanoparticles. Currently, the cellular internalization mechanism of THC by C6 cells remains unknown. We speculate the low cellular transport of free THC into C6 cells may be related to the inherent cell resistance to THC. However, Tf-NPs-THC

can be rapidly internalized by C6 cells via an enhanced energy-dependent endocytosis induced by Tf. It is essential that the specific mechanism should be further investigated.

The main challenge in treating glioma lies in achieving efficient accumulation of drugs in the brain. Usually, drug penetration into the brain is greatly limited by the presence of the blood-brain barrier. Although DOX is reported to be one of the most effective anti-cancer drugs against glioma, its therapeutic effect is often restricted due to its severe adverse reactions and poor BBB penetration. Recently, receptor-mediated drug delivery, which was expected to effectively cross the BBB and enter tumor tissues through active transport mechanisms, has been the most promising approach to tackle these problems. To investigate the brain-targeted potency of transferrin-targeted nanoparticles, *in vivo* bio-distribution assay was conducted. The results (Figure 3E) indicated that transferrin-targeted nanoparticles presented greater progressive brain penetration efficiency *in vivo* than did free DOX due to the integrated effect

of EPR and transferrin receptor-mediated positive cell uptake. This increased accumulation in the brain could contribute to the higher therapeutic efficiency of DOX. Additionally, the cardiotoxicity of DOX can be reduced through transferrin-modified nanoparticles-mediated selective delivery. Furthermore, our *in vivo* anti-glioma studies showed that the RAD+Tf-NPs-DOX-THC group had the optimum anti-tumor effects (Figure 4A, 4B) with no notable evidence of systemic toxicity (Figure 4E).

Overall, the novel “smart” nanoparticles can be prepared using a robust method and exhibit multifunctional improvement including excellent tumor-targeting property, controllable release, and synergistic therapeutic strategy, as compared to the traditional monotherapy. Because it was a preliminary pilot study to explore the combined application of DOX, THC, and radiation, our study has several limitations, especially the lack of an exhaustive comparison between the various formulations. Nevertheless, the newly-developed nanoparticles have great potential in treating malignant glioma.

Conclusions

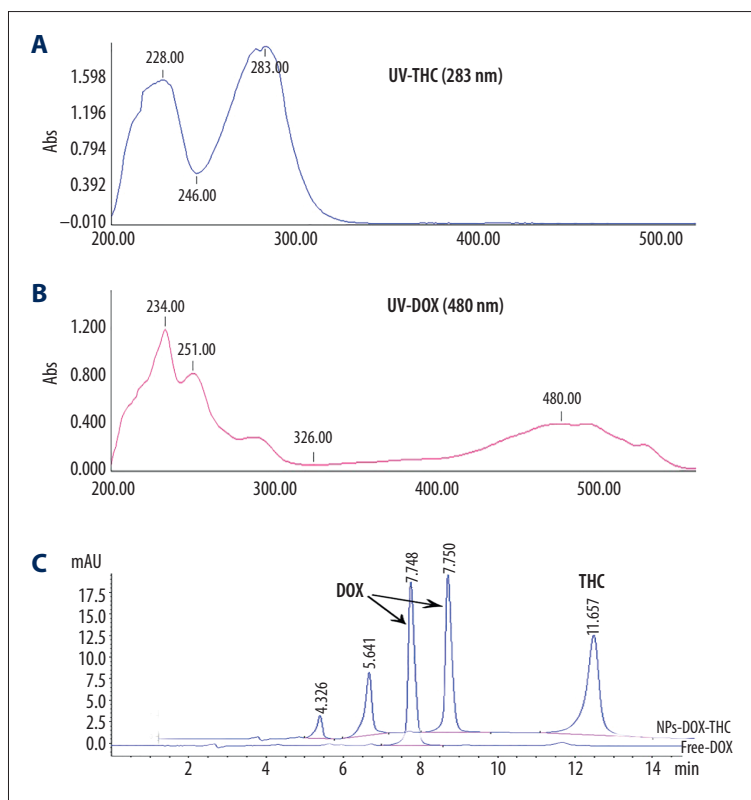
Transferrin-modified PEG-PLGA nanoparticles with pH-responsiveness were designed as a carrier of doxorubicin and

tetrahydrocurcumin for the synergistic chemoradiotherapy of glioma. Tetrahydrocurcumin as a radiosensitizer and doxorubicin as a chemotherapeutic were simultaneously incorporated into nanoparticles using the double-emulsion (W/O/W) method. The accelerated release of the loaded drug from Tf-NPs-DOX-THC was observed when exposed to acidic release medium, showing that the nanoparticles can rapidly release loaded drugs inside acidic cytoplasm. Tf-NPs-DOX can be efficiently taken up by C6 glioma cells and MCF-7 cells via transferrin receptor-mediated cells recognition. The enhanced *in vitro* anti-cancer activity of Tf-NPs-DOX-THC combined with radiation was confirmed by MTT, cell apoptosis, and clone formation assay. More importantly, Tf-NPs exhibited an enhanced drug accumulation in the brain compared with free DOX *in vivo*, and combined application of radiation and Tf-NPs-DOX-THC achieved favorable anti-tumor efficacy in both orthotopically-administered glioma nude mice and in subcutaneously-administered glioma nude mice. These results demonstrate that the combination of Tf-NPs-DOX-THC and radiation could be a promising strategy for the synergistic chemoradiotherapy of glioma.

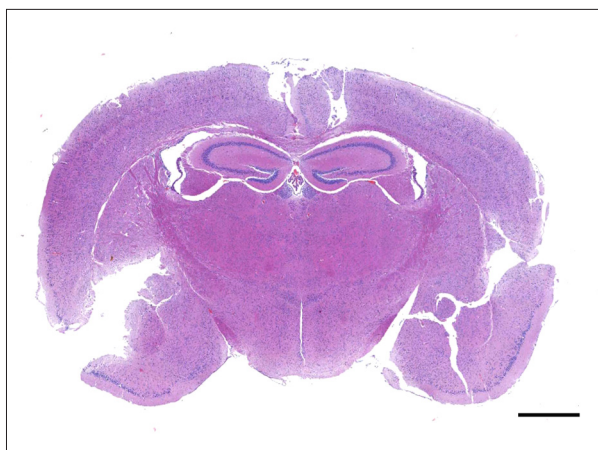
Conflict of interest

None.

Supplementary Data



Supplementary Figure 1. (A) and (B), UV scanning spectra of DOX and THC. (C) HPLC measurement of free DOX and NPs-DOX-THC. The results indicated that DOX and THC had been separated completely.



Supplementary Figure 2. Representative HE stained images of a normal brain. Scale bar: 1000 μm .

References:

- Guo J, Gao X, Su L et al: Aptamer-functionalized PEG-PLGA nanoparticles for enhanced anti-glioma drug delivery. *Biomaterials*, 2011; 32: 8010–20
- Zhao YZ, Lin Q, Wong HL et al: Glioma-targeted therapy using Cilengitide nanoparticles combined with UTMD enhanced delivery. *J Control Release*, 2016; 224: 112–25
- Yu B, Liu T, Du Y et al: X-ray-responsive selenium nanoparticles for enhanced cancer chemo-radiotherapy. *Colloids Surf B Biointerfaces*, 2015; 139: 180–89
- Liu H, Xie Y, Zhang Y et al: Development of a hypoxia-triggered and hypoxic radiosensitized liposome as a doxorubicin carrier to promote synergistic chemo-/radio-therapy for glioma. *Biomaterials*, 2017; 121: 130–43
- Caster JM, Yu SK, Patel AN et al: Effect of particle size on the biodistribution, toxicity, and efficacy of drug-loaded polymeric nanoparticles in chemo-radiotherapy. *Nanomed Nanotechnol*, 2017; 13: 1673–83
- Stupp R, Mason WP, van den Bent MJ et al: Radiotherapy plus concomitant and adjuvant temozolomide for glioblastoma. *New Engl J Med*, 2005; 352: 987–96
- Mäger I, Meyer AH, Li J et al: Targeting blood-brain-barrier transcytosis – perspectives for drug delivery. *Neuropharmacology*, 2016; 120: 4–7
- Kim K, Oh KS, Park DY et al: Doxorubicin/gold-loaded core/shell nanoparticles for combination therapy to treat cancer through the enhanced tumor targeting. *J Control Release*, 2016; 228: 141–49
- Liang B, Shahbaz M, Wang Y et al: Integrin $\beta 6$ -targeted immunoliposomes mediate tumor-specific drug delivery and enhance therapeutic efficacy in colon carcinoma. *Clin Cancer Res*, 2015; 21: 1183–95
- Jagetia GC: Radioprotection and radiosensitization by curcumin. *Adv Exp Med Biol*, 2007; 595: 301–20
- Yang G, Qiu J, Wang D et al: Traditional Chinese Medicine curcumin sensitizes human colon cancer to radiation by altering the expression of DNA repair-related genes. *Anticancer Res*, 2018; 38: 131–36
- Kang N, Wang MM, Wang YH et al: Tetrahydrocurcumin induces G2/M cell cycle arrest and apoptosis involving p38 MAPK activation in human breast cancer cells. *Food Chem Toxicol*, 2014; 67: 193–200
- Hong WU, Yan G, Wang S et al: [Curcumin modulates the radiosensitivity of gastric cancer cells by suppressing NF- κ B activity.] *J Shanxi Medical University*, 2014 [in Chinese]
- Qian Y, Ma J, Guo X et al: Curcumin enhances the radiosensitivity of U87 cells by inducing DUSP-2 up-regulation. *Cell Physiol Biochem*, 2015; 35: 1381–93 [Retracted article]
- Zhang X, Peng L, Liu A et al: The enhanced effect of tetrahydrocurcumin on radiosensitivity of glioma cells. *J Pharma and Pharmacol*, 2018; 70: 749–59
- Dhamecha D, Jalalpure S, Jadhav K et al: Doxorubicin loaded gold nanoparticles: Implication of passive targeting on anticancer efficacy. *Pharmacol Res*, 2016; 113: 547–56
- Li T, Zhang M, Wang J et al: Thermosensitive hydrogel co-loaded with gold nanoparticles and doxorubicin for effective chemoradiotherapy. *Aaps J*, 2016; 8: 146–55
- Zhang R, Jia X, Pei M, Liu P: Facile preparation of pH/reduction dual-responsive prodrug microspheres with high drug content for tumor intracellular triggered release of DOX. *React Funct Polym*, 2017; 116: 24–30
- Zhao D, Wu J, Li C et al: Precise ratiometric loading of PTX and DOX based on redox-sensitive mixed micelles for cancer therapy. *Colloids Surf B Biointerfaces*, 2017; 155: 51–60
- Li J, Yang H, Zhang Y et al: Choline derivate-modified doxorubicin loaded micelle for glioma therapy. *Acs Appl Mater Interfaces*, 2015; 7: 21589–601
- Byeon HJ, Thao le Q, Lee S et al: Doxorubicin-loaded nanoparticles consisted of cationic- and mannose-modified-albumins for dual-targeting in brain tumors. *J Control Release*, 2016; 225: 301–13
- Cui Y, Xu Q, Chow PK et al: Transferrin-conjugated magnetic silica PLGA nanoparticles loaded with doxorubicin and paclitaxel for brain glioma treatment. *Biomaterials*, 2013; 34: 8511–20
- Hu K, Shi Y, Jiang W et al: Lactoferrin conjugated PEG-PLGA nanoparticles for brain delivery: Preparation, characterization and efficacy in Parkinson's disease. *Int J Pharm*, 2011; 415: 273–83
- Li J, Feng L, Fan L et al: Targeting the brain with PEG-PLGA nanoparticles modified with phage-displayed peptides. *Biomaterials*, 2011; 32: 4943–50
- Mosafer J, Teymouri M, Abnous K et al: Study and evaluation of nucleolin-targeted delivery of magnetic PLGA-PEG nanospheres loaded with doxorubicin to C6 glioma cells compared with low nucleolin-expressing L929 cells. *Mater Sci Eng C Mater Biol Appl*, 2017; 72: 123–33
- Wang H, Zhao Y, Wu Y et al: Enhanced anti-tumor efficacy by co-delivery of doxorubicin and paclitaxel with amphiphilic methoxy PEG-PLGA copolymer nanoparticles. *Biomaterials*, 2011; 32: 8281–90
- Song G, Chao Y, Chen Y et al: All-in-One theranostic nanoplatfrom based on hollow TaOx for chelator-free labeling imaging, drug delivery, and synergistically enhanced radiotherapy. *Adv Funct Mater*, 2016; 26: 8243–54
- Wang Y, Liu P, Duan Y et al: Specific cell targeting with APRPG conjugated PEG-PLGA nanoparticles for treating ovarian cancer. *Biomaterials*, 2014; 35: 983–92
- Leopold LF, Tóдор IS, Diaconeasa Z et al: Assessment of PEG and BSA-PEG gold nanoparticles cellular interaction. *Colloids Surf A Physicochem Eng Asp*, 2017; 532: 70–76
- Agrawal P, Singh RP, Sonali et al: TPGS-chitosan cross-linked targeted nanoparticles for effective brain cancer therapy. *Mater Sci Eng C Mater Biol Appl*, 2017; 74: 167–76
- Daniels TR, Delgado T, Helguera G, Penichet ML: The transferrin receptor part II: Targeted delivery of therapeutic agents into cancer cells. *Clin Immunol*, 2006; 121: 159–76

32. Calzolari A, Larocca LM, Deaglio S et al: Transferrin receptor 2 is frequently and highly expressed in glioblastomas. *Transl Oncol*, 2010; 3: 123–34
33. Zhang X, Yang X, Ji J et al: Tumor targeting strategies for chitosan-based nanoparticles. *Colloids Surf B Biointerfaces*, 2016; 148: 460–73
34. Wei L, Guo XY, Yang T et al: Brain tumor-targeted therapy by systemic delivery of siRNA with Transferrin receptor-mediated core-shell nanoparticles. *Int J Pharm*, 2016; 510: 394–405
35. Karimi M, Ghasemi A, Sahandi Zangabad P et al: Smart micro/nanoparticles in stimulus-responsive drug/gene delivery systems. *Chem Soc Rev*, 2016; 45: 1457–501
36. Mura S, Nicolas J, Couvreur P: Stimuli-responsive nanocarriers for drug delivery. *Nat Mater*, 2013; 12: 991–1003
37. Ke CJ, Lin YJ, Hu YC et al: Multidrug release based on microneedle arrays filled with pH-responsive PLGA hollow microspheres. *Biomaterials*, 2012; 33: 5156–65
38. Du H, Liu M, Yu A et al: Insight into the role of dual-ligand modification in low molecular weight heparin based nanocarrier for targeted delivery of doxorubicin. *Int J Pharm*, 2017; 523: 427–38
39. Guo W, Li A, Jia Z et al: Transferrin modified PEG-PLA-resveratrol conjugates: *in vitro* and *in vivo* studies for glioma. *Eur J Pharmacol*, 2013; 718: 41–47
40. Zhang L, Shi Y, Song Y et al: Tf ligand-receptor-mediated exenatide-Zn(2+) complex oral-delivery system for penetration enhancement of exenatide. *J Drug Target*, 2018; 26(10): 931–40
41. Cai X, Yang X, Wang F et al: Multifunctional pH-responsive folate receptor mediated polymer nanoparticles for drug delivery. *J Biomed Nanotechnol*, 2016; 12: 1453–62
42. Ogawa D, Ansari K, Nowicki M et al: MicroRNA-451 Inhibits migration of glioblastoma while making it more susceptible to conventional therapy. *Noncoding RNA*, 2019; 5(1): pii: E25
43. Vishnu P, Roy V: Safety and efficacy of nab-Paclitaxel in the treatment of patients with breast cancer. *Breast Cancer*, 2011; 5: 53–65
44. Alexis F, Pridgen E, Molnar LK, Farokhzad OC: Factors affecting the clearance and biodistribution of polymeric nanoparticles. *Mol Pharm*, 2008; 5: 505–15
45. Yang X, Cai X, Yu A et al: Redox-sensitive self-assembled nanoparticles based on alpha-tocopherol succinate-modified heparin for intracellular delivery of paclitaxel. *J Colloid Interf Sci*, 2017; 496: 311–26
46. Fan Y, Wang Q, Lin G et al: Combination of using prodrug-modified cationic liposome nanocomplexes and a potentiating strategy via targeted co-delivery of gemcitabine and docetaxel for CD44-overexpressed triple negative breast cancer therapy. *Acta Biomater*, 2017; 62: 257–72
47. Cui Y, Xu Q, Chow PK et al: Transferrin-conjugated magnetic silica PLGA nanoparticles loaded with doxorubicin and paclitaxel for brain glioma treatment. *Biomaterials*, 2013; 34: 8511–20
48. Yu C, Gao C, Lu S et al: Facile preparation of pH-sensitive micelles self-assembled from amphiphilic chondroitin sulfate-histamine conjugate for triggered intracellular drug release. *Colloids Surf B Biointerfaces*, 2014; 115: 331–39
49. Zhang H, Xu J, Xing L et al: Self-assembled micelles based on Chondroitin sulfate/poly (d,l-lactide-co-glycolide) block copolymers for doxorubicin delivery. *J Colloid Interface Sci*, 2016; 492: 101–11
50. Yue J, Liu S, Mo G et al: Active targeting and fluorescence-labeled micelles: Preparation, characterization and cellular uptake evaluation. *J Control Release*, 2011; 152: 258–60